Hindawi
Advances in Materials Science and Engineering
Volume 2022, Article ID 6596464, 10 pages
https://doi.org/10.1155/2022/6596464

Research Article

Shrinkage and Warpage Mechanism of Overflow Water-Assisted Injection Molding Short Fiber-Reinforced Polymers

Huang DongYou,[1,2] **Liu Hesheng**,[1,3] **Kuang TangQing**,[3] **and Zhang Wei**[1]

[1]*Polymer Processing Laboratory, Nanchang University, Nanchang 330031, China*
[2]*Jiaxing Management Center of Primary and Secondary School Teacher Training, Jiaxing Education Institute, Jiaxing 314051, China*
[3]*School of Mechanical & Electrical Engineering, East China Jiaotong University, Nanchang 330013, China*

Correspondence should be addressed to Liu Hesheng; hsliu@vip.163.com

Received 29 March 2022; Revised 20 September 2022; Accepted 26 September 2022; Published 15 October 2022

Academic Editor: Guoqiang Xie

Copyright © 2022 Huang DongYou et al. This is an open access article distributed under the Creative Commons Attribution License, which permits unrestricted use, distribution, and reproduction in any medium, provided the original work is properly cited.

Experimental study on the shrinkage of short fiber-reinforced polymer injection molding products during the overflow water-assisted injection molding (OWAIM) process, and and analysis of the influence of process parameters with the computer-aided engineering (CAE) were performed. The investigation shows that the shrinkage of the product increases linearly along the melt flow with the increase of water injection pressure. The shrinkage of products is on the rise with the increase of water injection pressure, melt temperature, and mold temperature, but it is decreasing with the increase of flow delay time and fiber mass content. Based on the Taguchi orthogonal array design, an experiment study was conducted to characterize the effect of processing parameters on the shrinkage of OWAIM pipe. The results show that decreasing the mold temperature and increasing the fiber mass content can effectively reduce the shrinkage and warpage of products, thus improving the product quality.

1. Introduction

Based on the gas-assisted injection molding (GAIM) with water instead of gas as molding medium, the water-assisted injection molding (WAIM) technology is another new and potential fluid-assisted injection molding technology, which has attracted widespread attention for its unique forming advantages. The advantages of WAIM can be briefly described as follows: (1) as the water is incompressible, high-pressure water pushes the high temperature polymer melt forward to form hollow or partially hollow products to penetrate more steadily, its inner surface is smoother and its RWT is more uniform [1–5]. (2) As to fluid media, the water thermal conductivity is 40 times higher than the nitrogen gas and its heat capacity is 4 times higher than the nitrogen gas, so the WAIM can get better cooling effect and greatly shorten the molding cycles [6–11].

WAIM has been widely investigated in industry and academia. As a new fluid-assisted molding (FAIM) technology, how to reasonably control the WAIM processing parameters is valid to reduce the shrinkage. Up to now, great efforts have been made toward the simulation and investigation of the shrinkage of the product. Based on the research of pure resin WAIM, Wang et al., Andriyana et al., and Pawlak et al. [12–14] found the performance of reinforced polymer shows that fiber-reinforced polymer composites can not only improve the mechanical properties of polymer matrix, but also enhance mechanical properties and reduce mass of the product. Zhou et al. [15, 16] confirmed that fiber orientation and fiber length can improve obviously the mechanical properties of short glass-fiber reinforced polypropylene (SGFRPP) products. Li et al. [17] confirmed that other elements in the glassy matrix can effectively enhance its mechanical properties. With the deepening of the research, the breakthrough of shrinkage of plastic parts has been made in the measurement method and the influence of molding process [18, 19]. Wu et al. [20] found the shrinkage of polystyrene products decreased in the case of

very low holding pressure and very little time. Based on the influence of dwell pressure, pressure time, and melt temperature on polypropylene (PP) shrinkage, the study shows that the dwell pressure has the greatest contribution to the shrinkage, [21] and with the increase of dwell pressure, PP shrinkage becomes smaller [22–24]; increasing the injection temperature, the PP shrinkage will gradually decrease [25, 26]; with increasing pressure retention time, PP shrinkage decreases [27, 28]. Choi and Im [29] found that injection molding will make the crystalline polymer molecular chain closely arranged and orderly, after the residual stress and cooling, continuous crystallization to further reduce the size of the products, resulting in increased shrinkage. Kwon et al. [30] pointed out that because the polymer molecular chain, chain segments, and crystal polymer will be arranged in a specific direction, under the action of the melt shear movement, the size of the product is smaller; and the increase of molecular weight will reduce the lateral shrinkage of the product.

Many researchers have reported that the glass fiber (GF)-enhanced PP process can reduce the molding shrinkage of PP, [31, 32] with the increase of GF content, the longitudinal shrinkage rate becomes smaller. When 30% GF is added, the molding shrinkage rate of PP material decreases from 1.67% to 0.34% [33]. Nowadays, GF-enhanced PP has become an effective way to improve the molding shrinkage of PP materials. In order to solve the warpage of WAIM hollow products, in this paper, studying on a long straight round automobile cooling water pipe with the CAE technology and analyzing the shrinkage mechanism of OWAIM short fiber-reinforced polymer and experiment, which provided a theoretical basis to product of high-quality polymer products.

2. Numerical Simulation Method

In order to improve the accuracy of the calculation results, numerical simulations were performed. In this paper, a three-dimensional long straight round pipe with a section diameter of 16 mm and a main cavity length of 245 mm is constructed. The Moldex3D software is used to simulate the WAIM of the short fiber-reinforced polymer straight round pipe, create the mesh model where the middle is a regular tetrahedron and the boundary is a flat triangular structure. As shown in Figure 1, the 3D product mesh model is discretized with 5 layers, the node distance of 1.0 mm and 370237 elements.

In order to converge the calculation and conform the actual molding conditions, the boundary conditions are listed as follows:

(1) The melt velocity of the inlet is equal to the water injection velocity, and the melt pressure of the inlet is equal to the water injection pressure:

$$\begin{cases} u = 0, P = 0\left(t < t_{\text{de lay}}\right), \\ u = u_{\text{in}} = u_{\text{water}}, P = P_{\text{in}} = P_{\text{water}}\left(t \geq t_{\text{de lay}}\right). \end{cases} \quad (1)$$

(2) At the outlet, the front end of the melt communicates with the atmosphere, belongs to a free surface:

$$P = P_{out} = 0. \quad (2)$$

(3) There is no slip phenomenon between the melt and the mold wall:

$$U = 0. \quad (3)$$

(4) In the normal direction of adjacent fluid interface, the flow velocity, shear stress, and heat flow are continuous:

$$\begin{cases} u_{\alpha,1} \cdot n_{\alpha,1} = u_{\alpha+1,2} \cdot n_{\alpha+1,2}, \\ \sigma_{\alpha,1} \cdot n_{\alpha,1} + \sigma_{\alpha+1,2} \cdot n_{\alpha+1,2} = 0, \\ T_{\alpha,1} = T_{\alpha+1,2}, q_{\alpha,1} = q_{\alpha+1,2}. \end{cases} \quad (4)$$

The first subscript α shows the fluid in term α, which starts from the core and increases from the outside; the second subscript indicates the inner and outer surface of the fluid, 1 indicates the outer surface of the fluid itself and 2 indicates the inner surface of the fluid itself.

In the initial state, the type cavity front end is filled with the melt. After a short delay time, the high-pressure water is injected into the melt core to penetrate the melt with minimal flow resistance, forming a cross-sectional hollow plastic piece.

The Cross-WLF viscosity model [34] can characterize the melt viscosity in the WAIM, which includes seven parameters, as shown in Table 1.

3. Experimentation

3.1. Equipment Step. A lab-developed experimental platform for the OWAIM process was set up [35]. It consisted of an injection molding machine, a mold with changeable inserts, a water injection unit, and a mold temperature controller. The molding machine is fully automatic injection molding machine (TTI-250FT; Donghua Machinery Co., Ltd., China). The main cavity in the changeable inserts is the same diameter of 16 mm and the length of 245 mm, its end with overflow cavity (as shown in Figure 2). Water injection unit includes a water pump with a maximum pressure of 20 MPa, a water tank, and a water injector. The mold temperature controller (BTM-09W; Borack Machinery Co., Ltd., China) could controll the mold temperature from room temperature to 120°C.

3.2. Geometry of the Cavities, Shrinkage Measurement, and Fiber Orientation Observation. As shown in Figure 3, a long straight round pipe was chosen as the test case, which was used to investigate the influences of the processing parameters on the shrinkage. Taking 12 vertical sections ($P1$, $P2$, . . ., Pi, . . ., and $P12$) along the direction of the flow of the high-pressure water and measuring the external diameter (R_1, R_2, R_3, and R_4) at 4 positions on each section. The external diameter of the section Pi is defined as follows:

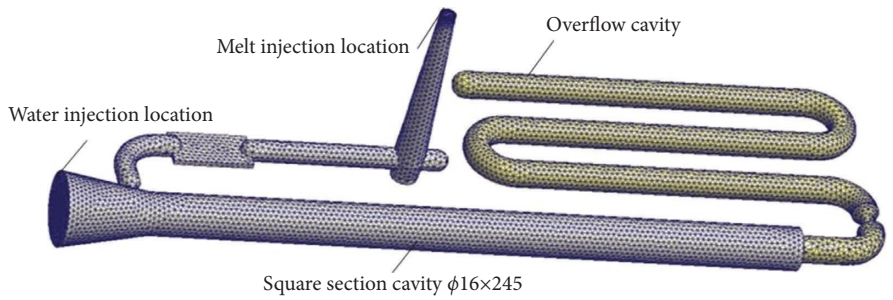

Figure 1: 3D product mesh model.

Table 1: The parameters of Cross-WLF viscosity model.

n	τ^* (Pa)	D_1 (Pa·s)	D_2 (K)	D_3 (K/Pa)	A_1	$\tilde{A}_2$ (K)
0.20426	33086.7	4.58E + 20	263.15	0	40.388	51.6

Figure 2: The main cavity mold.

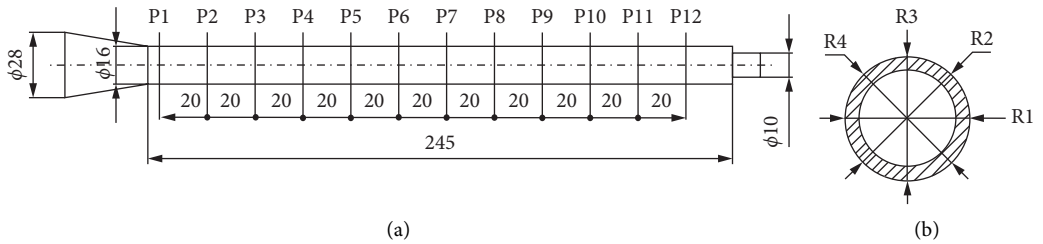

Figure 3: Cross-sectional locations and positions for measurement, (a) cross-sectional locations and (b) positions for measurement.

$$D_i = \frac{1}{4}\left(R_{i,1} + R_{i,2} + R_{i,3} + R_{i,4}\right), \tag{5}$$

where D_i is obtained by averaging the measured value of the four quartering points around the cross section of the position (as shown in Figure 3(b)).

In order to improve the accuracy of product measurement, under the same process parameters, three samples were prepared that the average value of each sample size was measured twice. The shrinkage of the section Pi is defined as follows:

$$S_i = \frac{D_0 - D_i}{D_0} \times 100\%, \tag{6}$$

where D_0 denotes dimensions of the mold cavity and D_i denotes dimensions of the test specimen.

In the direction perpendicular to the water flow, with the liquid-solid phase change, the translational invariance of the particles in the melt is disturbed, and the shrinkage after grain restructuring are consistent as the radial variables of the vertical section, which can reveal the internal mechanism of warpage deformation of the product.

A 5 mm long straight round pipe shut sample was taken at P1, P6, and P11, cut into two half rings in the flow direction, one half ring was taken and cooled in the liquid nitrogen vessel for 20 min, removed, fixed the section on the carrier, metal spraying, and finally observed by scanning electron microscope (SEM, Nova Nano SEM 450, FEI Co., Ltd., Chech).

3.3. Materials. According to the basic date of engineering plastics, the material of product is determined as PP with SGF mass content (SB224-2, SB224-3, and SB224-4) provided by LyondellBasell Co., Ltd., Germany, and the PP (PR340R) provided by PetroChina Lanzhou Petrochemical Co., Ltd., China, as shown in Table 2.

3.4. Orthogonal Experimental and Optimization Analysis. The impact of the short fiber-reinforced polymer WAIM technology on the quality of the final molding products includes many parameters, such as process parameters, material parameters, and structural parameters. In this study, according to the results of the research group, [36, 37] after the high-pressure water penetrated the melt, the influence of water injection pressure, water injection delay time, melt temperature, mold temperature, and fiber mass content on the shrinkage of products was studied, which each factor was at 4 levels in the orthogonal experiment. These process parameters are shown in Table 3.

In order to accurately investigate the influence of process parameters on the shrinkage of short fiber-reinforced polymer OWAIM products, the orthogonal experimental scheme was designed according to the table, which is 16 group analysis-experiments of cross-flow were carried out with the shrinkage of the front sections as the evaluation index. The experimental orthogonal table and experimental results are shown in Table 4.

From the range analysis results of Table 3, it can be seen that the order of the factors affecting the shrinkage of the front section is DEABC, that is, the mold temperature and fiber mass content are the main factors, and the melt temperature has the smallest effect. The shrinkage at the front of the penetration zone can be reduced by decreasing the mold temperature and increasing the fiber mass content.

As shown in Figure 4, it can be seen that the optimal combination of the minimal shrinkage is $A_1B_4C_1D_1E_4$, that is, the water injection pressure is 4 MPa, water injection delay time is 5 s, melt temperature is 210°C, mold temperature is 35°C, fiber weight percentage is 40%.

4. Results and Discussion

To understand the shrinkage of SGFRPP in the process of OWAIM, the basic parameters have chosen the PP matrix composite with 20% fiber percentage at melt temperature 230°C, water injection pressure 8 MPa, water injection delay time 1 s, and mold temperature 45°C. Under the basic processing parameters, an experimental sample was produced by OWAIM (as shown in Figure 5). By adjusting the process parameters, different shrinkage will occur at different positions along the axial direction (polymer melt flow direction), and show a linear increase.

4.1. Effects of Process Parameters on the Shrinkage of Products. Water Injection Pressure: The water injection pressure is controlled from 4 MPa to 10 MPa, and the pressure increases by 2 MPa. As shown in Figure 6, with the increase of the water injection pressure, the pipe shrinkage rate shows an upward trend. When the water injection pressure is 4 MPa, the shrinkage of the pipe is the smallest, which is close to 1.5%. When the water injection pressure reaches 10 MPa, the minimum shrinkage of the pipe has exceeded 2.2%. Because the increase of water injection pressure will accelerate the flow of the melt, resulting in intense shear movement, the axial and radial shrinkage is not synchronized. The molecular orientation is more obvious, and it is easy to increase the shrinkage rate. In order to reduce the shrinkage and the warping deformation of the pipe fittings, the water injection pressure can be properly controlled at 4 MPa on the basis of ensuring the stability of the melt flow.

Melt Temperature: Figure 6(b) showed that when the melt temperature is controlled between 210°C and 270°C and the temperature increase is 20°C, the shrinkage along the melt flow direction shows an upward trend. Because of that, the front part of melt always cools rapidly and forms a thicker solidified layer. In general, the shrinkage near the gate is less than 2.5%, but with the increase of melt temperature, the shrinkage of the pipe gradually increases. Because with the increase of melt temperature, the melt viscosity decreases continuously, the melt flow is accelerated, and the heat brought by water flow is compensated to the front part of the melt in time, which delays the cooling, resulting in larger change range and thinner RWT. When the melt temperature is set at 230°C, the shrinkage of the range is between 1.3% and 2.0%, the change range is the smallest, and the warpage is the smallest, too.

Mold Temperature. The mold temperature is controlled between 35°C and 65°C, and the temperature increase is 10°C. As shown in Figure 6(c), with the increase of mold temperature, the shrinkage rate shows an upward trend. When the mold temperature reaches 65°C, the shrinkage of the whole pipe section is in a high state, close to 6%; when the mold temperature is 35°C, the shrinkage of the whole pipe section is less than 1.5%. From the freezing of the gate to the demolding forming, with the temperature of the mold increases, the cooling rate of the pipe fitting slows down, the cooling time is extended, the time for molecular relaxation is more abundant, and the crystallinity is improved, while the high-temperature polymer melt (core layer) inside the pipe fitting is relatively thick, and the shrinkage rate is large. As a result, it is easier to form a penetration phenomenon inside. Therefore, we should reduce the mold temperature as much as possible to improve the quality of pipes.

Water Injection Delay Time: The water delay time between 0 s and 5 s were selected to conduct the experimented investigations. The results were shown in Figure 6(d), with

Table 2: Characteristics of polypropylene-based short fiber composites.

Characteristic parameters	PP	20% SGFPP	30% SGFPP	40% SGFPP
Melt flow rate (230°C/2.16 kg)	22 g/10 min	6.0 g/10 min	5.0 g/10 min	3.0 g/10 min
Density (23°C)	0.9 g/cm^3	1.03 g/cm^3	1.12 g/cm^3	1.21 g/cm^3
Tensile stress at yield	25.3 MPa	50.0 MPa	61.0 MPa	73.0 MPa
Flexural modulus	1017 MPa	3300 MPa	4700 MPa	5900 MPa
Notched izod impact strength (23°C)	5.0 kJ/m^2	14 kJ/m^2	18 kJ/m^2	19 kJ/m^2

Table 3: Levels of factors used in experiments.

Factors	Levels			
	1	2	3	4
A: water injection pressure (MPa)	4	6	**8**	10
B: water injection delay time (s)	0	**1**	3	5
C: melt temperature (°C)	210	**230**	250	270
D: mold temperature (°C)	35	**45**	55	65
E: fiber mass content (%)	0	**20**	30	40

Table 4: $L_{16}(4^5)$ orthogonal array used in experiment and results.

Experiment no	Factors					Shrinkage (%)
	A	B	C	D	E	
1	1	1	1	1	1	0.8752
2	1	2	2	2	2	1.0428
3	1	3	3	3	3	1.6322
4	1	4	4	4	4	0.9624
5	2	1	2	3	4	0.8274
6	2	2	1	4	3	2.2398
7	2	3	4	1	2	0.9137
8	2	4	3	2	1	1.7386
9	3	1	3	4	2	3.1064
10	3	2	4	3	1	2.9872
11	3	3	1	2	4	0.4183
12	3	4	2	1	3	0.6554
13	4	1	4	2	3	4.2614
14	4	2	3	1	4	0.3840
15	4	3	2	4	1	3.2385
16	4	4	1	3	2	1.3641
RWT $\Sigma(1)/4$	1.128	2.268	1.224	0.707	2.210	
$\Sigma(2)/4$	1.430	1.663	1.441	1.865	1.607	
$\Sigma(3)/4$	1.792	1.551	1.715	1.703	2.197	
$\Sigma(4)/4$	2.312	1.180	2.281	2.387	0.648	
R	1.184	1.088	1.057	1.680	1.562	

the increase of the water injection delay time, the shrinkage of the pipe gradually decreased. It was due to the heat transfer across the cavity wall, and the melt near the wall had a higher viscosity. The high-pressure water pushes the melt more slowly, leading to a slower penetration speed, as well as the flow viscosity of the melt was higher at the drag flow area, so the shrinkage rate tended to be stable for the solidification layer at the wall. When the delay time of water injection is 0 s, the shrinkage rate of the product increases from 2.3% to 2.9% along the main cavity. The main reason is that, in the former stage of the main cavity, the viscosity and flow resistance of the melt have little changes, but the cooling degree of the melt in the front and rear ends is obviously different, which further enlarges the thickness deviation between the front section and the rear section.

4.2. Effects of Fiber Mass Content on Shrinkage of Products. Based on the basic parameters, Figure 7 shows how the PP-based composites with different fiber mass contents behave in terms of the distribution of fiber orientation along the flow direction and the shear rate distribution. It can be seen from Figure 7 that with the increasing fiber content, the fiber orientation of the three positions in P1, P6, and P11 along the melt flow direction was significantly increased. At P1, the fiber orientation of the 20% SGFRPP pipe is not high, the 30% SGFRPP pipe fiber orientation is significantly increased, and the 40% SGFRPP pipe fiber orientation is the most obvious. At P6, the fiber orientation was also increased as the fiber content increased from 20% to 40%. At P11, the fiber orientation along the melt flow direction decreased, but the 40% SGFRPP pipe fiber orientation remained the most pronounced.

It can be seen from Figure 8 that when the PP is used, the shrinkage rate at the end of the pipe is the largest, which is close to 7%; the shrinkage rate of the PP pipe with 20% fiber content along the melt flow direction is less than that of the pure PP pipe; the minimum shrinkage rate of the PP pipe is close to the maximum shrinkage rate of 20% SGFRPP pipe. The shrinkage rate of 30% SGFRPP pipe is close to that of 20% SGFRPP pipe, but the average of its shrinkage rate is less than that of 20% SGFRPP pipe. The maximum shrinkage rate of 40% SGFRPP pipe is less than that of 30% SGFRPP pipe.

As the fiber content increases, the melt viscosity is also increasing, constantly increasing the flow resistance, intensifying the mutual interference between the fibers, so that the fiber orientation of the melt shell and the channel layer is significantly increased during the melt injection stage. However, in the high-pressure water injection stage, the dense fibers reinforce each other, making the melt produce intense shear movement along the radial direction, decreasing the fiber orientation distribution in the rear stage of the main cavity, resulting in the thinning of the RWT, which causes the shrinkage rate of the product increases rapidly. In the injection molding process, with the

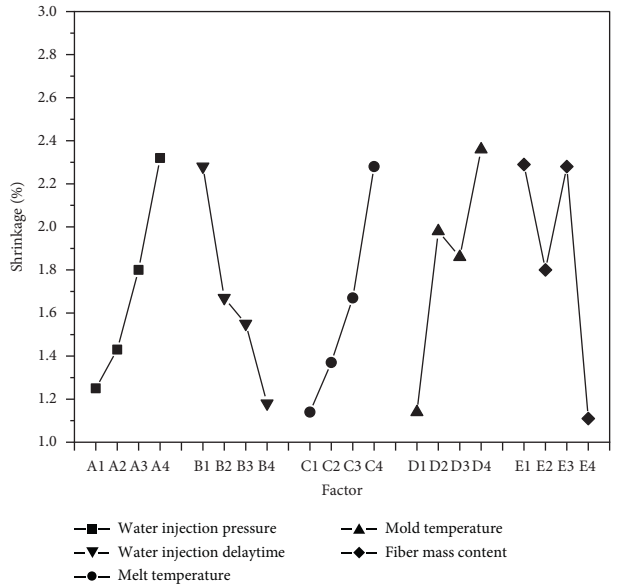

Figure 4: Effects of factors on shrinkage.

Figure 5: The OWAIM specimen.

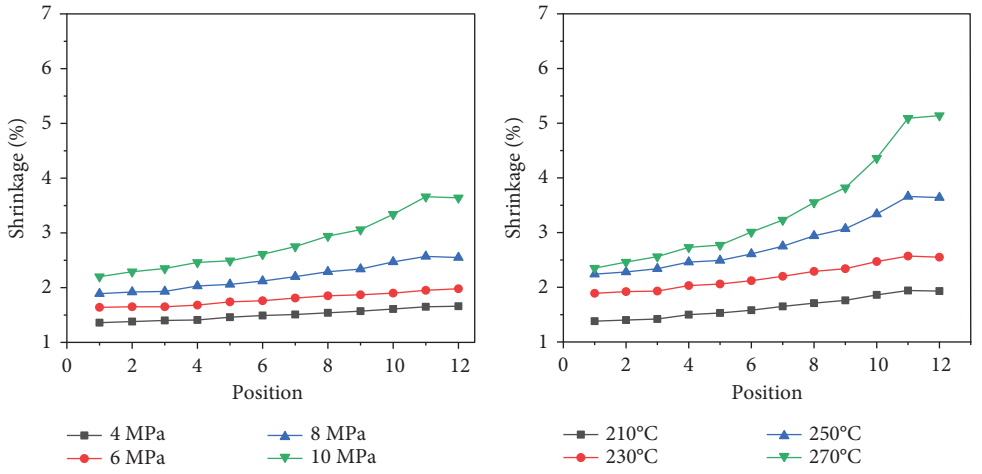

Figure 6: Continued.

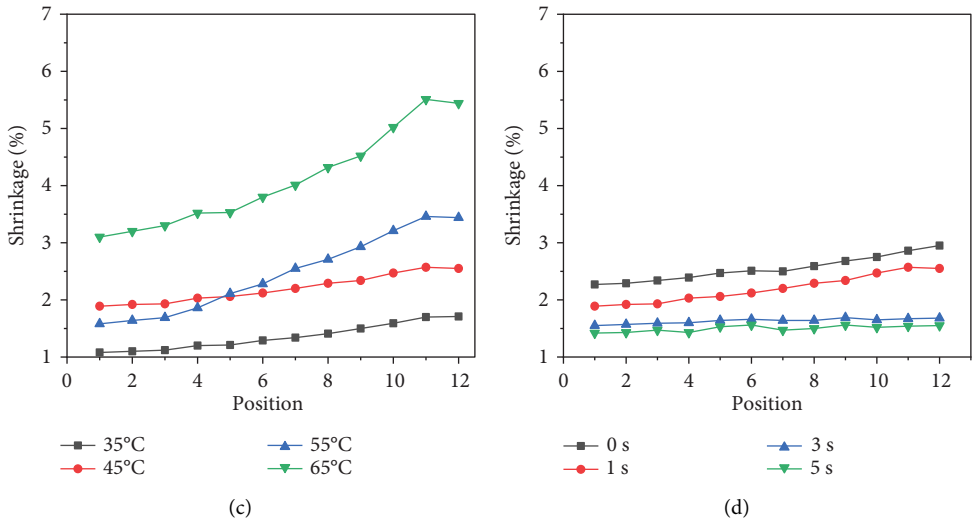

Figure 6: Effects of process parameters on shrinkage of WAIM 20% SGFRPP products, (a) water injection pressure, (b) melt temperature, (c) mold temperature, and (d) water injection delay time.

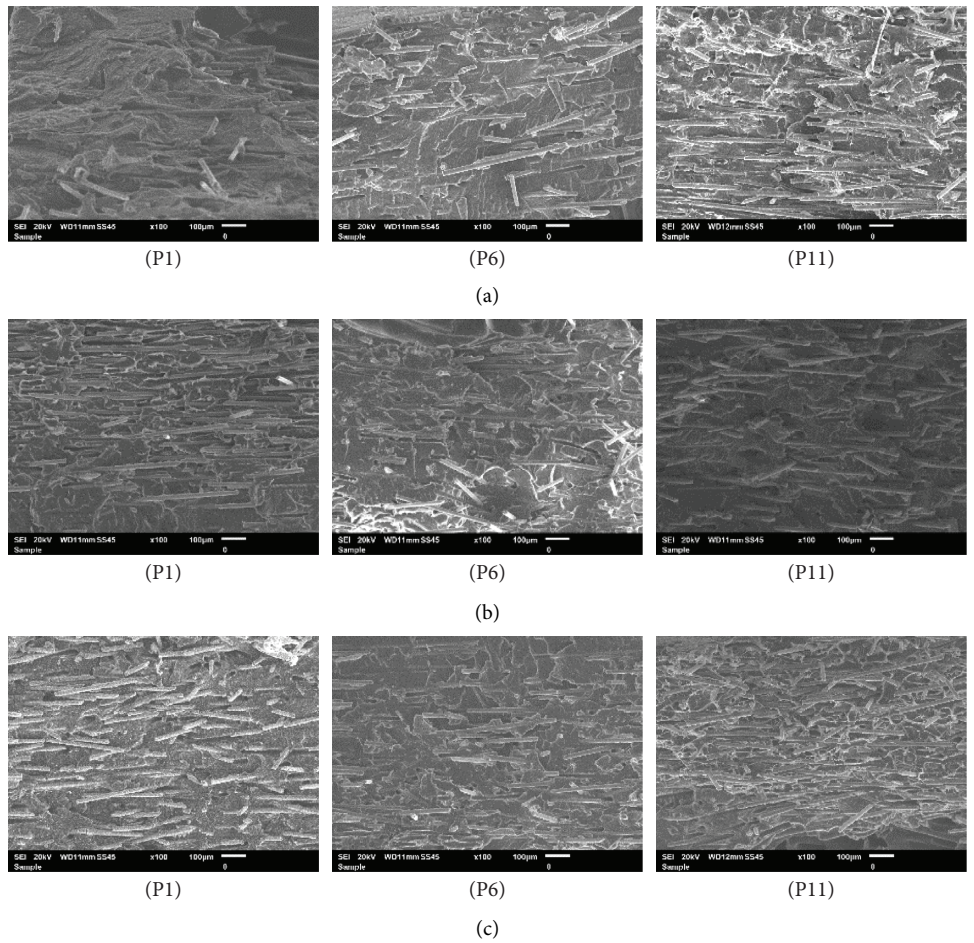

Figure 7: Fiber orientation distribution of different fiber mass content along the flow direction, (a) SEM images of 20% GFRPP, (b) SEM images of 30% GFRPP, and (c) SEM images of 40% GFRPP.

addition of glass fiber, the fiber orientation enhances the anisotropy of the melt, which increases the viscosity of the polymer melt, improves the plasticizing ability of the pipe and the heat distortion temperature of PP, thus inhibiting the shrinkage of the pipe and reducing the molding shrinkage of PP.

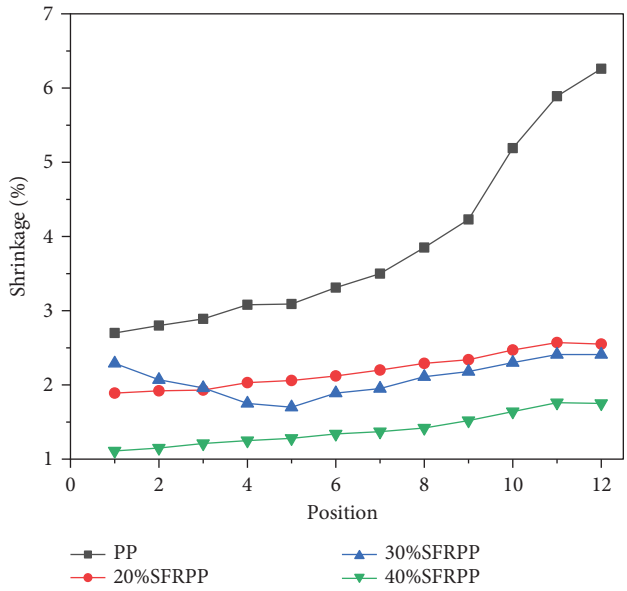

Figure 8: Effects of fiber mass content on the shrinkage of OWAIM pipes.

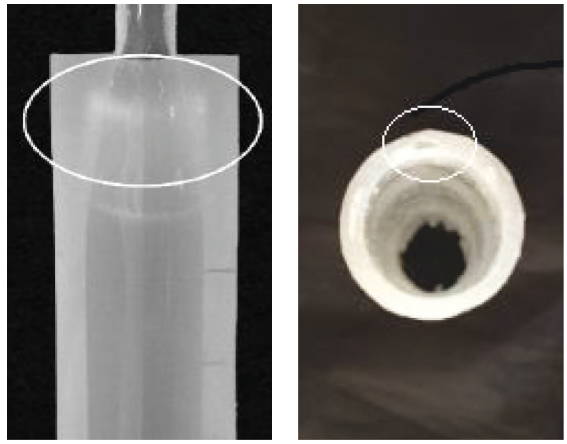

Figure 9: OWAIM to form holes caused by cooling shrinkage at end position, (a) the melt accumulation and (b) the concave holes.

4.3. Analysis of the Shrinkage of End Sections. It can be seen from Figure 9 that, in the OWAIM, the shrinkage rate of the initial section of the SFRPP pipe is the smallest, but the shrinkage effect of the final section is obvious, which is easy to form the phenomenon of melt accumulation. The main reason is that there is a sudden change in the cross section of the transition area between the end of the pipe and the overflow cavity, resulting in uneven cooling of the melt, a large shrinkage, and forming a "dead zone" at this sudden change in the cross section. The cooling time of the melt at the end position is relatively long before the high-pressure water push, the shell layer, and the water channel layer of the melt are basically solidified, and the RWT is relatively thick. As shown in Figure 9(b), under the high-pressure water push, the high temperature polymer melt enters the overflow cavity forward, and the water channel layer becomes thinner, which accelerates the cooling contraction of the high temperature melt in the melt core layer to produce large tensile stress and form concave holes, seriously affecting the quality of products. When the shrinkage of the melt is large, a large tensile stress will be generated. If the tensile stress is too large at this time, the melt in the water channel layer will be broken, which causes high-pressure water enters the melt, resulting in secondary penetration [38].

5. Conclusion

The shrinkage rate is an important index of the OWAIM. The effect of different process parameters on the shrinkage rate of products was analyzed by experiments, and the shrinkage mechanism of the OWAIM straight pipe was discussed by volume numerical simulation. The main conclusions are as follows:

(1) The main factors affecting the shrinkage of products are the mold temperature and the fiber content, that is, reducing the mold temperature and increasing the fiber content can reduce the shrinkage of products, thereby improving the quality of products.

(2) In the OWAIM, the optimal combination of factors for the minimum shrinkage of the product is $A_1B_4C_1D_1E_4$, that is, the water injection pressure is 4 MPa, the water injection delay time is 5 s, the melt temperature is 210°C, the mold temperature is 35°C, and the fiber weight percentage is 40%, which causes the smallest warpage.

(3) Compared with the PP products, under the complex action of fiber orientation, the short glass fiber-reinforced OWAIM technology can greatly reduce the shrinkage and improve the mechanical properties of the products.

Data Availability

The data used to support the findings of this study are available from the corresponding author upon request.

Conflicts of Interest

The authors declare that they have no conflicts of interest.

Acknowledgments

This work forms part of a project supported by the National Natural Science Foundation of China (NSFC, no. 21664002, no. 51563010, no. 52163006), the industrial field of Science and Technology Department of Jiangxi Province (no. 20203BBE53065), and the Natural Science Foundation of Jiangxi Province (no. 2018BAB206014).

References

[1] J. H. Zheng, J. P. Qu, and N. Q. Zhou, "Advance in the research of the water-assisted injection molding technology," *Engineering Plastics Application*, vol. 31, no. 7, pp. 65–68, 2003.

[2] W. Michaeli, T. Juntgen, and A. Brunswick, "WIT-En route to series production: first industrial application of the water injection technique," *Kunststoffe Plast Europe*, vol. 91, no. 3, pp. 37–39, 2001.

[3] S. J. Liu and Y. S. Chen, "Water-assisted injection molding of thermoplastic materials: effects of processing parameters," *Polymer Engineering & Science*, vol. 43, no. 11, pp. 1806–1817, 2003.

[4] C. T. Huang, W. H. Yang, M. H. Tsai, and K. I. Lu, "The investigation of flow behavior of polymeric melts in the water assisted injection molding," in *Proceedings of the 62nd Annual Technical Conference of SPE*, pp. 566–569, SPE/ANTEC, Chicago, IL, USA. Brookfield, May 16-20,2004.

[5] A. Z. Ahmadzai and A. H. Behravesh, "An experimental investigation on water penetration in the process of water assisted injection molding of polypropylene," *Polimery*, vol. 54, no. 07/08, pp. 564–572, 2009.

[6] S. J. Liu, "Water assisted injection molding: a review," *International Polymer Processing*, vol. 24, no. 4, pp. 315–325, 2009.

[7] W. Michaeli, A. Brunswick, and C. Kujat, "Reducing cooling time with water-assisted injection moulding-Advantages over gas-assisted injection," *Kunststoffe-Plast Europe*, vol. 90, no. 8, pp. 67–72, 2000.

[8] P. Mapleston, "Injection molding water-assisted process shows promise," *Modern Plastics International*, vol. 31, no. 1, p. 33, 2001.

[9] S. J. Liu and W. K. Chen, "Experimental investigation and numerical simulation of cooling process in water assisted injection moulded parts," *Plastics, Rubber and Composites*, vol. 33, no. 6, pp. 260–266, 2004.

[10] J. G. Yang, X. H. Zhou, and Q. Niu, "Residual wall thickness study of variable cross-section tube in water-assisted injection molding," *International Polymer Processing*, vol. 27, no. 5, pp. 584–590, 2012.

[11] S. Sannen, P. Van Puyvelde, and J. De Keyzer, "Defect occurrence in water-assisted injection-molded products: definition and responsible formation mechanisms," *Advances in Polymer Technology*, vol. 34, no. 1, Article ID 21746, 2015.

[12] L. X. Wang, Y. Li, and W. G. Zhuang, "Influence of processing parameters and fiber content on shrinkage of fiber-reinforced PP injection-molded part," *Polymer Materials Science and Engineering*, vol. 25, no. 9, pp. 135–137+141, 2009.

[13] A. Andriyana, N. Billon, and L. Silva, "Mechanical response of a short fiber-reinforced thermoplastic: experimental investigation and continuum mechanical modeling," *European Journal of Mechanics - A: Solids*, vol. 29, no. 6, pp. 1065–1077, 2010.

[14] F. Pawlak, M. Aldas, J. López-Martínez, and M. D. Samper, "Effect of different compatibilizers on injection-molded green fiber-reinforced polymers based on poly(lactic acid)-maleinized linseed oil system and sheep wool," *Polymers*, vol. 11, no. 9, p. 1514, 2019.

[15] Y. G. Zhou, B. Su, and L. S. Turng, "Mechanical properties, fiber orientation, and length distribution of glass fiber-reinforced polypropylene parts: influence of water-foaming technology," *Polymer Composites*, vol. 39, no. 12, pp. 4386–4399, 2018.

[16] B. Su and Y. G. Zhou, "Influence of foaming technology on fibre breakage in long fibre-reinforced polypropylene composites parts," *Plastics, Rubber and Composites*, vol. 46, no. 8, pp. 365–374, 2017.

[17] K. Li, L. X. Liang, P. Du et al., "Mechanical properties and corrosion resistance of powder metallurgical Mg-Zn-Ca/Fe bulk metal glass composites for biomedical application," *Journal of Materials Science & Technology*, vol. 103, no. 103, pp. 73–83, 2022.

[18] D. Annicchiarico and J. R. Alcock, "Alcock.Review of factors that affect shrinkage of molded part in injection molding," *Materials and Manufacturing Processes*, vol. 29, no. 6, pp. 662–682, 2014.

[19] N. Ranjbar, M. Mehrali, A. Behnia et al., "A comprehensive study of the polypropylene fiber reinforced fly ash based geopolymer," *PLoS One*, vol. 11, no. 1, Article ID e0147546, 2016.

[20] Y. C. Wu, Y. H. Cui, H. L. Jin, and C. C. Ning, "Study on the preparation and thermal shrinkage properties of nano-SiO_2/UHMWPE/HDPE blend microporous membranes," *Journal of Applied Polymer Science*, vol. 132, no. 3, Article ID 41321, 2015.

[21] O. Mohd Hilmi, S. Hasan, W. N. A. W. Muhammad, and Z. Zuramashana, "Optimising injection moulding parameter setting in processing polypropylene-clay composites through taguchi method," *Applied Mechanics and Materials*, vol. 271-272, pp. 272–276, 2012.

[22] K. M. B. Jansen, "Measurement and prediction of anisotropy in injection moulded PP products," *International Polymer Processing*, vol. 13, no. 3, pp. 309–317, 1998.

[23] K. M. B. Jansen, D. J. Van Dijk, and M. H. Husselman, "Effect of processing conditions on shrinkage in injection molding," *Polymer Engineering & Science*, vol. 38, no. 5, pp. 838–846, 1998.

[24] S. J. Liao, D. Y. Chang, H. J. Chen et al., "Optimal process conditions of shrinkage and warpage of thin-wall parts," *Polymer Engineering and Science*, vol. 44, no. 5, pp. 917–928, 2004.

[25] A. Mamat, T. F. Trochu, and B. Sanschagrin, "Analysis of shrinkage by dual kriging for filled and unfilled polypropylene molded parts," *Polymer Engineering and Science*, vol. 35, no. 19, pp. 1511–1 520, 1995.

[26] W. C. Bushko and V. K. Stokes, "Solidification of thermo-viscoelastic melts. Part II: effects of processing conditions on shrinkage and residual stresses," *Polymer Engineering and Science*, vol. 35, no. 4, pp. 365–383, 1995.

[27] F. D. Santis, R. Pantani, V. Speranza, and G. Titomanlio, "Analysis of shrinkage development of a semicrystalline polymer during injection molding," *Industrial & Engineering Chemistry Research*, vol. 49, no. 5, pp. 2 469–472 476, 2010.

[28] M. Altan, "Reducing shrinkage in injection moldings via the taguchi, ANOVA and neural network methods," *Materials & Design*, vol. 31, no. 1, pp. 599–604, 2010.

[29] D. S. Choi and Y. T. Im, "Prediction of shrinkage and warpage in consideration of residual stress in integrated simulation of injection molding," *Composite Structures*, vol. 47, no. 1-4, pp. 655–665, 1999.

[30] K. Kwon, A. Isayev, K. Kim, C. Van Sweden, H. Kim, and V. Sweden, "Theoretical and experimental studies of anisotropic shrinkage in injection moldings of semicrystalline polymers," *Polymer Engineering & Science*, vol. 46, no. 6, pp. 712–728, 2006.

[31] M. Fujiyama, "Structures and properties of injection moldings of glass fiber-filled polypropylenes," *International Polymer Processing*, vol. 8, no. 3, pp. 245–254, 1993.

[32] A. J. Pontes, N. M. Neves, J. C. Velosa, A. R. Faria, and A. S. Pouzada, "Glass fiber contents of PP plates and their properties. Part I: shrinkage and changes in time[J]. Materials Science and Engineering," pp. 230–232, 2002.

[33] X. A. Lou, J. Y. Su, C. M. Meng, and H. Duan, "Research on shrinkage of modified polypropylene," *China Plastics*, vol. 25, no. 12, pp. 59–62, 2011.

[34] A. Gava and G. Lucchetta, "Numerical simulation of a PA66 flow behaviour in a hot runner gate," *Macromolecular Symposia*, vol. 263, no. 1, pp. 53–66, 2008.

[35] F. Yang, T. Q. Kuang, W. Liu, and H. S. Liu, "Distribution of residual wall thickness of water projectile assisted injection molding pipes with curved sections," *Polymer Materials Science and Engineering*, vol. 33, no. 11, pp. 112–118, 2017.

[36] T. Q. Kuang, Q. Feng, P. Xu, D. Lai, and K. S. Liu, "Influence of glass fiber contents on the residual wall thickness and microscopic morphology of water-assisted injection molding pipes of short-glass-fiber reinforced polypropylene composites," *Polymer Materials Science and Engineering*, vol. 36, no. 2, pp. 105–111, 2020.

[37] T. Q. Kuang, J. Y. Pan, Q. Feng et al., "Residual wall thickness of water-powered projectile-assisted injection molding pipes," *Polymer Engineering & Science*, vol. 59, no. 2, pp. 295–303, 2019.

[38] K. M. B. Jansen, R. Pantani, and G. Titomanlio, "As-molded shrinkage measurements on polystyrene injection molded products," *Polymer Engineering & Science*, vol. 38, no. 2, pp. 254–264, 1998.